MARTIN MARIETTA ENERGY SYSTEMS LIBRARIES
3 4456 0154173 7

ORNL/TM-10285

ornl

OAK RIDGE NATIONAL LABORATORY

MARTIN MARIETTA

Controlled Nucleation and Growth Studies in Metal Oxide and Alkoxide Systems by Dynamic Laser-Light-Scattering Methods

C. H. Byers
R. R. Brunson
M. T. Harris
D. F. Williams

OAK RIDGE NATIONAL LABORATORY
CENTRAL RESEARCH LIBRARY
CIRCULATION SECTION
4500N ROOM 175
LIBRARY LOAN COPY
DO NOT TRANSFER TO ANOTHER PERSON
If you wish someone else to see this report, send in name with report and the library will arrange a loan.

OPERATED BY
MARTIN MARIETTA ENERGY SYSTEMS, INC.
FOR THE UNITED STATES
DEPARTMENT OF ENERGY

Printed in the United States of America. Available from
National Technical Information Service
U.S. Department of Commerce
5285 Port Royal Road, Springfield, Virginia 22161
NTIS price codes—Printed Copy: A04 Microfiche A01

This report was prepared as an account of work sponsored by an agency of the United States Government. Neither the United States Government nor any agency thereof, nor any of their employees, makes any warranty, express or implied, or assumes any legal liability or responsibility for the accuracy, completeness, or usefulness of any information, apparatus, product, or process disclosed, or represents that its use would not infringe privately owned rights. Reference herein to any specific commercial product, process, or service by trade name, trademark, manufacturer, or otherwise, does not necessarily constitute or imply its endorsement, recommendation, or favoring by the United States Government or any agency thereof. The views and opinions of authors expressed herein do not necessarily state or reflect those of the United States Government or any agency thereof.

ORNL/TM-10285

Chemical Technology Division

CONTROLLED NUCLEATION AND GROWTH STUDIES IN METAL OXIDE AND ALKOXIDE SYSTEMS BY DYNAMIC LASER-LIGHT-SCATTERING METHODS

C. H. Byers
R. R. Brunson
M. T. Harris
D. F. Williams

Date of Issue - April 1987

Prepared by the
OAK RIDGE NATIONAL LABORATORY
Oak Ridge, Tennessee 37831
operated by
MARTIN MARIETTA ENERGY SYSTEMS, INC.
for the
U.S. DEPARTMENT OF ENERGY
under contract DE-AC05-84OR21400

MARTIN MARIETTA ENERGY SYSTEMS LIBRARIES
3 4456 0154173 7

CONTENTS

	Page
LIST OF FIGURES	v
LIST OF TABLES	vii
ABSTRACT	1
1. INTRODUCTION	1
2. DYNAMIC LIGHT-SCATTERING THEORY	5
3. BACKGROUND ON SILICA CRYSTALLIZATION	16
4. EXPERIMENTAL APPARATUS AND PROCEDURE	20
5. RESULTS AND DISCUSSION	25
6. CONCLUSIONS	39
7. NOMENCLATURE	39
8. REFERENCES	41

LIST OF FIGURES

Figure		Page
1	Typical behavior of the autocorrelation function (A^*) of a periodic signal (A)	9
2	Typical results from a dynamic light-scattering experiment	13
3	Chromia particles formed by homogeneous precipitation in aqueous solution. Conditions: stock F62; temperature = 70°C; aging = 32 h	17
4	Hematite particles formed by homogeneous precipitation in aqueous solution, 0.07 x 0.02 μm	18
5	Dynamic light-scattering spectrometer for high-temperature experiments	21
6	Operation of high-temperature spectrometer	22
7	Effects of NH_3 and H_2O on silica growth in ethanol medium	26
8	Colloidal silica produced by controlled hydrolysis in ethanol (Stöber process). Conditions: stock F91; temperature = 25°C	27
9	Size distribution	28
10	Intensity of scattered light (large and small particles)	30
11	Dilution of silica suspensions with ethanol and NH_3-ethanol	31
12	Effect of solvent on silica growth rate	34
13	Silica particles formed by hydrolysis of TEOS in *tert*-butyl alcohol	35
14	Hydrolysis of TEOS-Run 41; variation of wt % ETOH and particle volume with time	37
15	Hydrolysis of TEOS-Run 41; first-order kinetics	38

LIST OF TABLES

Table		Page
1	Effects of initial reactant concentrations on ultimate diameter of the particles	32

CONTROLLED NUCLEATION AND GROWTH STUDIES IN METAL OXIDE AND ALKOXIDE SYSTEMS BY DYNAMIC LASER-LIGHT-SCATTERING METHODS

C. H. Byers, R. R. Brunson, M. T. Harris, and D. F. Williams

ABSTRACT

A method for studying the dynamics of crystallization by using an in situ crystallizer in a dynamic laser-light-scattering system has been developed at the Oak Ridge National Laboratory. Results for growing systems in the size range of 0.005 to 1 μm may be monitored nondestructively using this method. In a series of tests, homogeneous precipitation techniques provide reproducible, controlled nucleation and growth of oxides such as hematite and silica. The effects of driving force and homogeneous and heterogeneous seeding were compared with a theoretical treatment of crystal formation and growth. The hydrolysis of tetraethoxysilicate (TEOS) in ethanol, n-butanol, and tert-butyl alcohol was investigated as a function of initial water and ammonia contents. Ethanol concentration, particle size, and number concentration were studied as a function of time. Preliminary results indicate that in the presence of excess water the growth rate of silica particles has a first-order dependence on TEOS concentration.

1. INTRODUCTION

The fundamental aspects of nucleation and growth kinetics in crystallization form the basis for the understanding of a broad class of processes that are important in energy-related systems. For instance, crystallization and precipitation are a significant part of typical processing systems in the nuclear fuel cycle.[1,2] In conventional chemical operations,

crystallization is a well-known purification method in which more art than science is generally utilized. More complete knowledge concerning the basic mechanisms associated with nucleation and crystal growth will allow improvements in plant design and subsequent manufacturing operations, which will result in better control and greater energy efficiency.

A central focus in the development of a new generation of ceramics for use under extreme conditions has been on gaining additional information about the chemical factors that control the production of powders suitable for the tailoring of superior properties.[3] Generally, the base materials are precipitated metal oxides, such as silica, which are either drawn from natural sources or obtained synthetically. The latter approach leads to better, more reproducible properties in the resulting ceramic. One of the key factors associated with success in this field is the production of monodisperse powders in the submicron range. Equally important is the ability to control and characterize the material as it is produced.[4]

Much of the chemical engineering literature in the areas of nucleation and crystal growth is directed at polydisperse systems consisting of relatively large crystals.[5,6] To date, most of the theory has been directed toward these problems. At best, one may generally expect only short-range applicability of predictive correlations. Certainly, caution should be exercised in extending the predictions for one type of equipment to different, but similar, devices. In proceeding from one chemical species to another, one cannot rely on data taken on the original system. That is, correlations generally apply only to a

single chemical system, and one must repeat experiments for each new chemical moiety.

Improvement in the state of the theory is generally inhibited by the complexity of the processes involved in typical crystallization phenomena. Normal studies involve complex systems whose growth depends on a number of factors, not all of which can be controlled or, in some cases, can be identified. The phenomena that control nucleation and growth most often occur at the size level of nuclei or small crystals (0.003- to 0.1-μm region); yet, as a result of limitations in methods of observing particles, crystal growth is normally observed in the size range above 1 μm. Further, because of experimental limitations, populations of crystals with a wide size distribution are invariably studied. A number of assumptions about population dynamics are necessary before any analysis may be made of this type of experimental data. Thus, a better understanding of the fundamentals of nucleation and crystal growth may be obtained if nucleation and crystallization can be followed during nucleation and early growth (0.001 to 1 μm) and the growth of monodisperse crystals is studied. The combination of the two aforementioned experimental goals will contribute information that will allow more detailed input to the development of an in-depth understanding of crystallization.

The most significant recent contributions to particle sizing in the past decade have stemmed from the development of laser-light scattering and its applications to the observation of submicron particles.[7] With goals that are somewhat different from those in the current study, a state-of-the-art laser-light scattering facility has been developed in

our laboratory.[8] The general concept involves the scattering of laser light in a vessel (usually a thermally controlled quartz cell). The scattering is observed with a photomultiplier tube, which is placed at an angle (from 6° to almost 180°) to the incident light. The scattered light from a seed material dispersed in an otherwise homogeneous medium will contain information on the Brownian motion of the particles, which allows us, through application of the Stokes-Einstein equation, to infer the average size of the seed material. This operation is performed with a digital correlator in which pulses from the photomultiplier tube are collected and an autocorrelation function is generated. Data are collected and stored in a dedicated computer, which serves a number of important functions, including data storage, data reduction, and control and programming of experiments. The entire process consumes less than 1 min in typical applications and produces accurate average size measurements from 0.005 to 1 μm.

In addition, the capability for quickly inferring particle aspect ratio and size distributions through variable angle studies and computer manipulation of the data by a Provencher analysis[9] is available. Laser-light scattering provides an excellent approach to observing crystals in a size range of considerable theoretical interest throughout a time scale of interest without intruding on the progress of the process.

The second area that is crucial to this work is the development of homogeneous nucleation. During the past 20 years, a group of workers at the Clarkson Institute of Technology, under the leadership of Professor Egon Matijevic, has developed precipitation and crystallization techniques in which a single burst of nuclei is formed in a

reactor.[10,11] The nucleation is followed by the growth of monodisperse crystals. The nucleation process is generally achieved by the careful heating of a metal salt in an acidic solution. Hydrolysis of the metal ions occurs, followed by deprotonation and formation of the "complex" nuclei precursors. At a critical concentration these complexes nucleate in a single burst, after which growth of the crystals never again allows the concentration to become sufficiently large to produce nuclei. Typical of such systems is a mixture of ferric chloride in dilute HCl. When heated to about 100°C, the ferric oxide crystals of uniform size are produced.

Another similar system, the hydrolysis of tetraethoxysilicate, was proposed by Van Helden.[12] In the current investigation, we report on the homogeneous precipitation reaction, which is the central feature of the hydrolysis system. Since this method is fairly generally applicable to the production of metal oxides, it is representative of a broad class of materials which are basic to the making of ceramics. The precautions that must be observed in such preparations are similar to those required in light-scattering experiments (i.e., purity, temperature control, and cleanliness). Thus, this method of producing crystals under carefully controlled conditions provides an outstanding opportunity for studying nucleation and growth in a relatively uncomplicated manner.

2. DYNAMIC LIGHT-SCATTERING THEORY

Light passing through a medium is scattered and is a direct consequence of dielectric fluctuations (heterogeneities) in the scattering medium. Light scattered in a perfectly homogeneous medium tends to interfere destructively such that no net scattered field is observed.

With properly controlled experiments, we can relate the scattered light signal to the physical properties that cause the fluctuations of the solution and the scattering disposition. In the case of colloidal particles suspended in a transparent fluid, Brownian motion is the phenomenon of interest.

Brownian motion can be observed in particles that are large (diameter, ~0.01 μm) relative to the molecular scale.[13-15] The intensity of scattered light from a fluid is greatly enhanced by the addition of colloidal (seed) particles, providing a valuable analytical tool for assessing size and shape of particles. As is shown here, light-scattering analysis may also be used to observe the dynamics of particle growth in a fluid.

Let us consider the particle motion as being maintained by collisions with molecules of the medium and retarded by the effect of viscous drag. The scattered light signal is modulated by the particle motion. The Brownian motion of a free particle (i.e., no applied force field) is described by the Langevin equation:[14]

$$\frac{d\bar{u}}{dt} = -\beta\bar{u} + \bar{A}(t) \quad , \tag{1}$$

where

$\bar{u}$ = particle velocity vector,

t = time,

β = coefficient of dynamic friction,

$\bar{A}(t)$ = fluctuating influence of molecular collision process characteristic of molecular Brownian motion.

For a spherical particle, the coefficient of dynamic friction is given by Stokes Law, as follows:

$$\beta = 6\pi a\eta/m \ , \tag{2}$$

where

a = particle radius,

η = fluid viscosity,

m = particle mass.

It is generally assumed that $\bar{A}(t)$ is a random variable (independent of $\bar{u}$) which varies on a much more rapid time scale than $\bar{u}(t)$. The solution to the Langevin equation is a probability distribution since $\bar{A}(t)$ is a stochastic variable. Therefore, the solution is a distribution, $W(\bar{u},t;\bar{u}_o)$, which specifies the probability of occurrence of velocity $\bar{u}$ at time t, given that $\bar{u} = \bar{u}_o$ at $t = t_o$. The constraint that W tend to a Maxwellian distribution in T (temperature of fluid) as $t \to \infty$ allows us to proceed with the solution. Since Eq. (1) is linear and of the first order,

$$\bar{u} - \bar{u}_o e^{-\beta t} = e^{-\beta t} \int_o^t e^{-\beta t'} A(t')dt' \ , \tag{3}$$

and

$$W(\bar{u},t;\bar{u}_o) = \left[\frac{m}{2\pi kT(1 - e^{-2\beta t})}\right]^{3/2} \exp\left[\frac{-m\left|\bar{u} - \bar{u}_o e^{-\beta t}\right|^2}{2kT(1 - e^{-2\beta t})}\right] . \tag{4}$$

Applying the statistical velocity behavior of a particle in Brownian motion yields the particle displacements since

$$\bar{r} - \bar{r}_o = \int_o^t \bar{u}(t)dt \ , \tag{5}$$

where

$\bar{r} - \bar{r}_o$ = displacement vector,

$\bar{r}$ = position vector at time t,

$\bar{r}_o$ = position vector at $t = t_o$.

For times much greater than β^{-1}, we find[14] that

$$W(\bar{r},t;\bar{r}_o,\bar{u}_o) = (4\pi Dt)^{-3/2} \exp\left(\frac{-|\bar{r} - \bar{r}_o|^2}{4Dt}\right) , \tag{6}$$

where

W = probability of particle suffering a displacement to $\bar{r}$ at time t, given that $\bar{u} = \bar{u}_o$ and $\bar{r} = \bar{r}_o$ at $t = t_o$;

$$D = kT/(6\pi a\eta). \tag{7}$$

The self-diffusion coefficient, D, was identified by Einstein;[16] thus, Eq. (7) is known as the Stokes-Einstein equation. The distribution function, W, will be useful in relating the particle motion to the light signal fluctuations.

Both the collection and the analysis of the scattered light signal in such a manner as to relate the signal fluctuations to the motion of the suspended particles are primary objectives. The basis for characterizing these fluctuations is the autocorrelation function (Fig. 1).

ORNL DWG 85-258

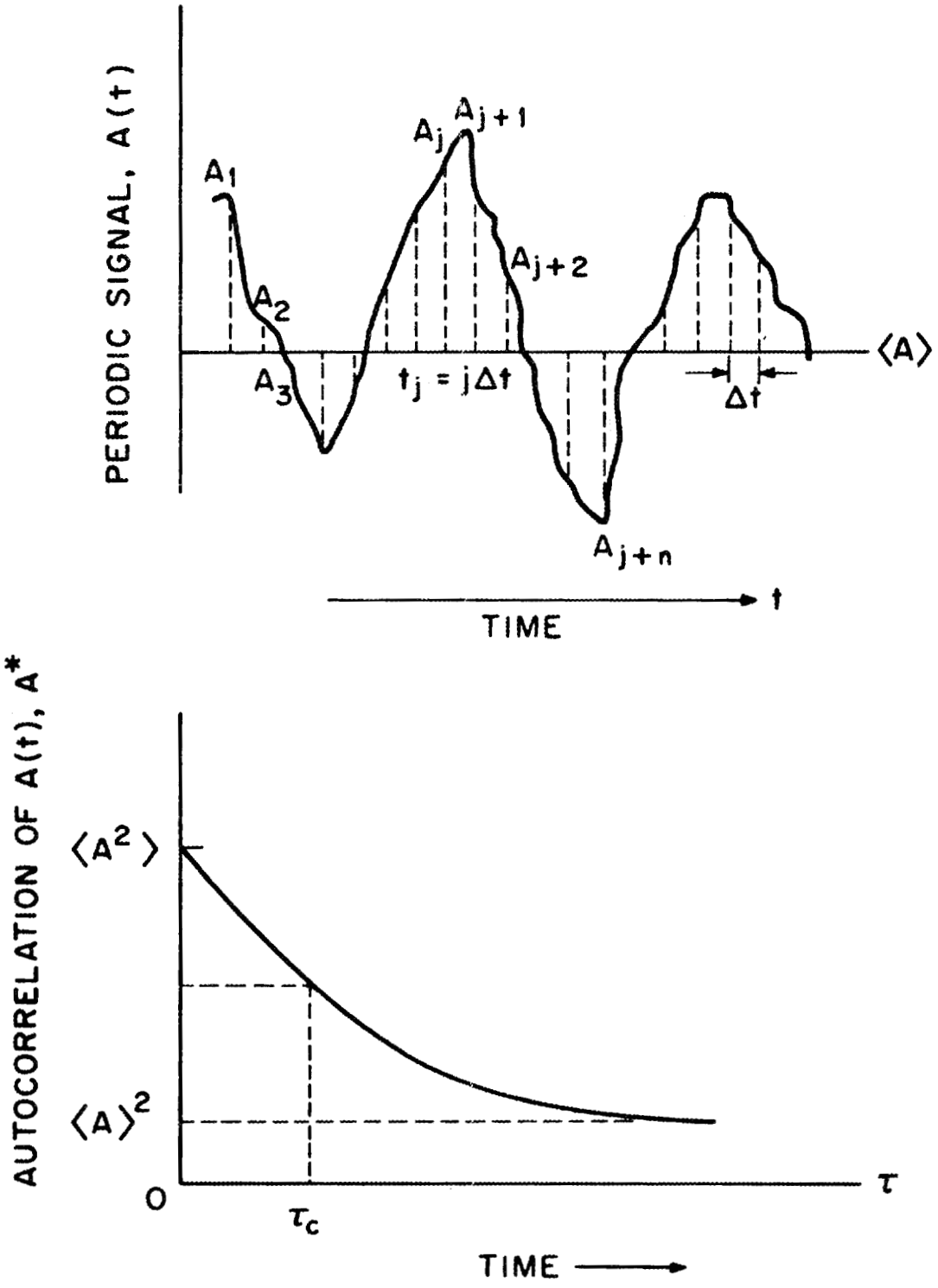

Fig. 1. Typical behavior of the autocorrelation function (A^*) of a periodic signal (A).

The autocorrelation function of a signal is defined as the time average of the product of signals (otherwise identical) displaced by time τ:

$$A^*_{(\tau)} = \text{autocorrelation function} \equiv \langle A(o)\ A(\tau)\rangle$$

$$\equiv \lim_{T\to\infty} \frac{1}{T} \int_o^T A(t)\ A(t+\tau)dt \cong \lim_{N\to\infty} \frac{1}{N} \sum_{j=1}^{N} A_j\ A_{j+n}\ , \tag{8}$$

and

$$\langle A\rangle = \text{time average of signal } A = \frac{1}{T} \int_o^T A(t)dt. \tag{9}$$

A useful property of this function is its ability to characterize the period of fluctuation of a signal (Fig. 1). For values of τ that are small compared with the signal period τ_s, $A(t) \sim A(t+\tau)$ and $A^* \sim \langle A^2\rangle$. For times $\tau \gg \tau_s$, $A(t)$ and $A(t+\tau)$ are not correlated in any special way and $A^* \sim \langle A(o)\ A(\tau)\rangle \sim \langle A(o)\rangle\ \langle A(\tau)\rangle = \langle A\rangle^2$. Since $\langle A^2\rangle$ is uniformly greater than $\langle A\rangle^2$, A^* will tend to decay from its maximum of $\langle A^2\rangle$ to its asymptotic ($T \to \infty$) value of $\langle A\rangle^2$ (Fig. 1).

The signal of interest in our system is the intensity (square of electric field = $E_s{}^2$) of the scattered light. By application of Maxwell's equations to our system, it is possible to show that the scattered electric field signal is proportional to[13]

$$E_s(t) \cong \sum_{j=1}^{N} \exp\ [i\bar{q} \cdot \bar{r}_j(t)]\ , \tag{10}$$

where

$\overline{r}_j(t)$ = position vector of jth particle at time t,

$\overline{q}$ = vector difference between incident and scattered propagation vectors,

$|\overline{q}| = \frac{4\pi n}{\lambda_i} \sin \frac{\theta}{2}$,

n = refractive index of the medium,

θ = scattering angle,

λ_i = incident wavelength.

The autocorrelation function of the scattered electric field is proportional to

$$A_s^*(t) \cong \sum_{j=1}^{N} \langle \exp\left(i\, \overline{q} \cdot [\overline{r}_j(t) - \overline{r}_j(o)]\right) \rangle \ , \tag{11}$$

where the sum j=1, . . . N is taken over particles present in the scattering volume at time t and t = 0.

It is evident that A_s^* is dependent on $[\overline{r}_j(t) - \overline{r}_j(o)]$ — the displacement of a particle in time t. This provides the link to Brownian motion theory. In order to deal mathematically with the summing of individual particle contributions, we must resort to calculating A_s^* based on properties averaged over the scattering medium and particle velocities.

Considering a generic particle, the normalized autocorrelation function of the scattered field is

$$A_s^*/N = \iint \exp\left(i\, \overline{q} \cdot (\overline{r}_j(t) - \overline{r}_j(o))\right) \cdot W(\overline{r},t;\overline{r}_o,\overline{u}_o) \cdot P(u_o)dr_o du_o \ , \tag{12}$$

where

W = factor used to predict the occurrence of a particle suffering displacement $\bar{r} - \bar{r}_o$ within time t, given $\bar{r} = \bar{r}_o$ and $\bar{u} = \bar{u}_o$ at $t = 0$ [Eq. (6)];

P = the Maxwellian velocity distribution, which is the factor used to predict the probability of a particle having velocity u_o at $t = 0$ and is equal to $\left(\frac{m}{2\pi kT}\right)^{3/2} \exp(-m\,|\,u_o\,|^2/2kT)$;

N = number of particles in scattering volume ~ constant.

Performing the integration over r_o and u_o and making appropriate numerical approximations yields[14,17]

$$A_s^* \cong \exp(-q^2Dt) = \exp(-t/\tau_c) \ , \tag{13}$$

where

$q = |\,\bar{q}\,| = 4\pi n \sin(\theta/2)/\lambda_i$,

D = diffusion coefficient = $kT/(6\pi a\eta)$,

τ_c = characteristic decay time = $(q^2D)^{-1}$.

Note that A_s^* is a decaying exponential function of time (Fig. 2).

Up to this point, our discussion has been restricted to the ideal case of monodisperse spherical particles; however, we know that no real systems are truly monodisperse. Even the widely used latex particles have a small, but appreciable, spread in size. It is important to consider the effect that polydispersity has on the data analysis. The signal from a polydisperse system contains a summation of exponentials, each with its own decay constant and associated scattering power:[18]

$$A_s^* = K \int_{r=0}^{r=\infty} [f(r) \cdot P(q,r) \cdot r^6 \cdot \exp(-t/\tau_i)]dr \ , \tag{14}$$

ORNL DWG 85-259

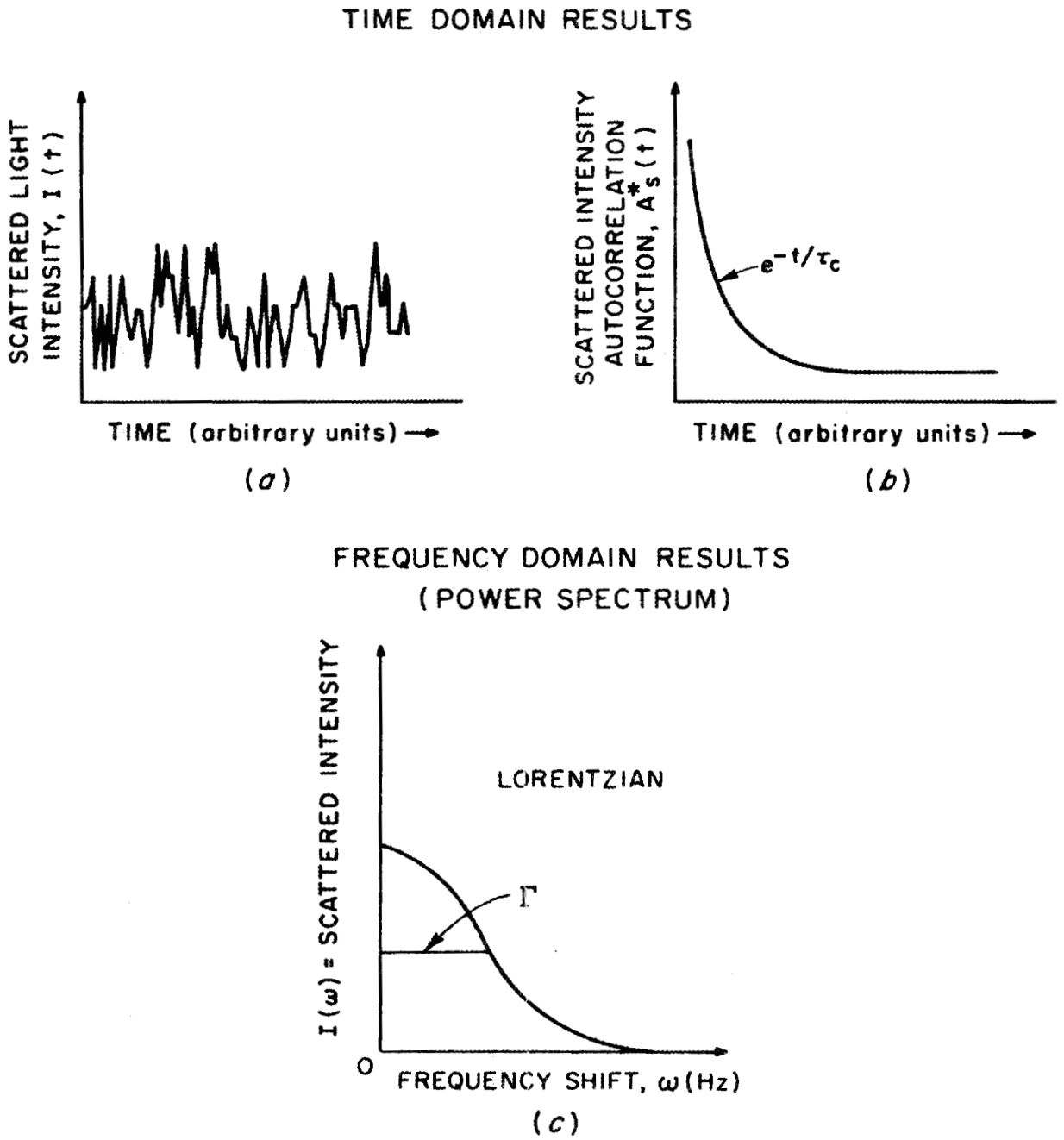

Fig. 2. Typical results from a dynamic light-scattering experiment.

where

r = particle radius,

$f(r)$ = normalized distribution of particle size,

$P(q,r)$ = Mie scattering factor, $P \sim 1$ for $r \ll \lambda$,

τ_i = decay time for $r = r_i$.

The exact solution requires inversion of this equation to yield $f(r)$ directly, an operation which is very difficult to do accurately for complex signals. As shown in Eq. (14), because of the scattering power's r^6 dependence, large particles are more easily detected than small ones.

The approach taken by many investigators is to analyze the signal in a simpler manner that provides useful results. The cumulants method is the most widely used technique.[19-21] This analysis leads to the following approximation for the autocorrelation function:

$$\ln(A_s^*) = -\bar{\Gamma}t + \frac{\mu_2 t^2}{2!} - \frac{\mu_3 t^3}{3!} + \ldots$$

$$= -\bar{\Gamma}t + \frac{1}{2!}\,\frac{\mu_2}{\bar{\Gamma}^2}\,(\bar{\Gamma}t)^2 - \frac{1}{3!}\,\frac{\mu_3}{\bar{\Gamma}^3}\,(\bar{\Gamma}t)^3 + \ldots \qquad (15)$$

The form of $\ln(A_s^*)$ is a polynomial in t with the coefficients representing different properties of the linewidth distribution. The linear and quadratic terms are the most significant and are readily measured in most experiments. The linear term is the average linewidth, as defined in Eq. (15). Since the scattering power of individual particles is skewed heavily toward large particles [Eq. (14)], this "average" Γ will result in "average" diameters weighted toward the largest species. This average linewidth has a more straightforward interpretation when applied to

measuring polymer diffusion coefficients.[19] The scattering is restricted to the Rayleigh regime (particle size << wavelength), and the scattered intensity is assumed to be proportional to the square of the molecular weight. This results in:

$$\frac{\overline{\Gamma}}{q^2} = \frac{\sum N_i M_i D_i}{\sum N_i M_i} = \overline{D}_z \ , \tag{16}$$

where

$\overline{D}_z$ = z average diffusion coefficient,

N_i = concentration of polymers with M_i,

M_i = molecular weight,

D_i = diffusion coefficient of polymer with $M = M_i$.

The second moment (μ_2) normalized by the square of the average linewidth ($\mu_2/\overline{\Gamma}^2$) provides us with a polydispersity parameter. For a perfect monodisperse suspension, $\mu_2/\overline{\Gamma}^2 = 0$. In practice, values of $\mu_2/\overline{\Gamma}^2$ less than 0.1 are taken as an indication of a narrow distribution.

It is readily apparent that a quadratic regression analysis of $\ln(A_s^*(t))$ vs t will provide estimates of $\overline{\Gamma}$ and $\mu_2/\overline{\Gamma}^2$. Using the Stokes-Einstein relation [Eq. (7)], we obtain the viscosity directly since

$$D = \overline{\Gamma}/2q^2 \tag{17}$$

and

$$d_p = kT/(3\Pi\mu D\eta) \ . \tag{18}$$

This relationship, which is widely used, forms the basis for the size analysis in the current work. In particular, it permits the crystal size to be measured as well as the polydispersity to be estimated. The chemistry associated with homogeneous precipitation is reviewed in Sect. 3.

3. BACKGROUND ON SILICA CRYSTALLIZATION

As stated earlier, one of the goals of our program is to observe crystallization and precipitation in as fundamental a manner as possible within the confines of producing worthwhile results. One means of ensuring simplicity is to make monodisperse particles. Matijevic and co-workers[22,23] have developed homogeneous precipitation as a means of producing monodisperse sols. During the course of his studies, he has made a wide variety of metal salts in both amorphous and crystalline forms. Figures 3 and 4 are electronmicrographs of examples of both forms which we prepared in our laboratories. Figure 3 shows a chromia sol which was formed by the hydrolysis of chromic chloride; it is apparently amorphous. On the other hand, hematite ($Fe_2O_3 \cdot 5H_2O$) produced by similar means has a crystalline structure. Using dynamic laser-light scattering, we have been able to observe the growth of both of these species.

Among the reactions in this class are the tetraethoxy metal compounds, with tetraethoxyorthosilane (TEOS) being the most widely studied moiety. The silica produced in the precipitation is of interest in the manufacture of glass and ceramics. TEOS readily hydrolyzes with water to yield ethanol and silica.

Since TEOS is insoluble, it is usually dissolved in ethanol or some other aliphatic alcohol. Hydrolysis with water alone is very slow indeed; thus, it is normal practice to use either an acid or ammonia to act as a catalyst. The former encourages the growth of gel structures, while the latter is a morphological catalyst producing spherical particles.[24] Stoichiometrically, the reaction proceeds as follows:

ORNL-PHOTO 6061-84

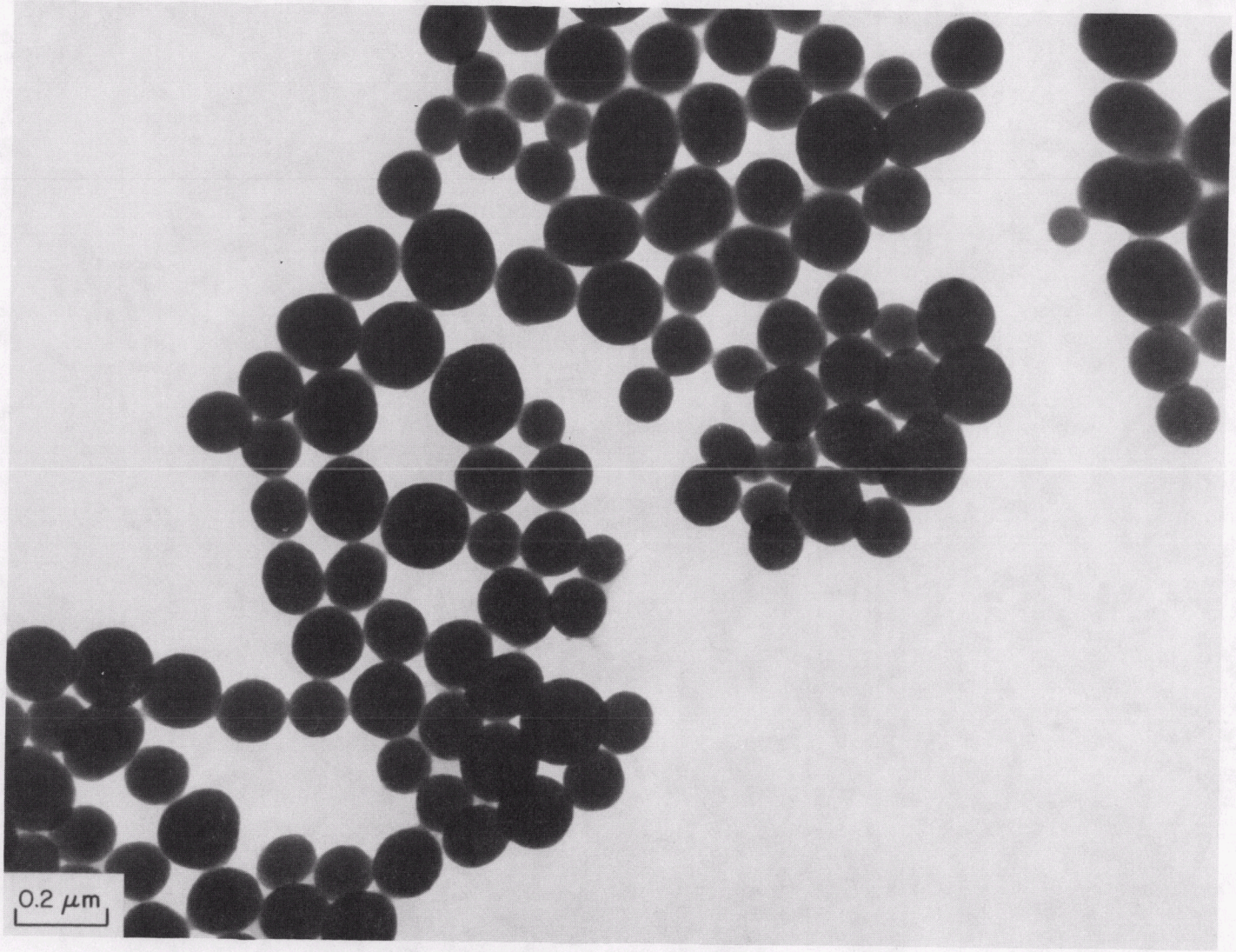

Fig. 3. Chromia particles formed by homogeneous precipitation in aqueous solution. Conditions: stock F62; temperature = 70°C; aging = 32 h.

ORNL-PHOTO 0391-84

Fig. 4. Hematite particles formed by homogeneous precipitation in aqueous solution, 0.07 x 0.02 μm.

$$Si\text{-}(OC_2H_5)_4 + 2H_2O \rightarrow SiO_2 + 4C_2H_5OH \ . \tag{19}$$

The reaction is actually a hydrolysis,

$$Si\text{-}(OC_2H_5)_4 + 4H_2O \rightarrow Si\text{-}(OH)_4 + 4C_2H_5OH \ , \tag{20}$$

followed by a condensation step,

$$Si\text{-}(OH)_4 \rightarrow SiO_2 + 2H_2O \ . \tag{21}$$

Polymerization-type reactions are also feasible, but these do not cause precipitation in the case of a deficiency of hydroxyl groups to complete the reaction. Evidence indicates that polymeric species remain in solution and are available for further reaction.[25]

Four primary chemical factors affect the kinetics of the reaction and the ultimate size of the solid spheres that are grown. The concentration of TEOS, the type of alcohol used as the solvent, the initial water concentration, and the amount of ammonia present all have significant effects on the process. All of these factors have been examined in varying degrees of sophistication by a number of workers in the area. The use of an alcohol as the solvent for the reaction leads to exchange reactions between the ethoxy groups of the TEOS and the alcohol.[26] This tendency is reduced as one proceeds from a primary to a secondary alcohol and completely disappears when a ternary alcohol is used. The medium also has an effect on the basic hydrolysis rate,[26] with the reaction being fastest in primary alcohols and slowest in ternary alcohols.

The two greatest influences on the rate of hydrolysis, and hence on the rate of precipitation, are the initial water concentration and the catalyst concentration. Stober, Fink, and Bohn[24] investigated these

influences, plotting final particle size as a function of the concentrations of the two species. At a 0.28-mol/L concentration of TEOS in ethanol, a maximum particle size of approximately 0.8 μm was produced when the concentrations of both water and ammonia were 7 mol/L each. The condensation rate is influenced profoundly by the water concentration, while the ammonia primarily affects the morphology. Changing the solvent to a higher-molecular-weight or a more branched structure leads to the production of larger particles, albeit more slowly. The actual observation of the growth of particles has been limited to emulsion polymerization studies.[27]

4. EXPERIMENTAL APPARATUS AND PROCEDURE

A custom-built dynamic light-scattering spectrometer is the centerpiece of this experiment. The apparatus (Figs. 5 and 6) consists of a laser, source optics, a sample enclosure, collection optics, a detector, and signal processing equipment. Except for the high-temperature enclosure, the specification and assembly of components were based on established guidelines.[17,18] The high-temperature enclosure was designed for another study and was replaced by a quartz spectrophotometer for the current work.

A 2-W argon-ion laser (Spectra Physics model 165-06) generates a vertically polarized beam (λ = 488 nm) that is focused by a 150-mm plano-convex lens onto the center of the sample cell. The beam is focused to a narrow width (~0.2 mm) in order to maximize the modulation of the scattered light (i.e., high signal/noise). The lens axis is adjusted so as to be coincident with the source beam by a micropositioner (Newport model LP-1). Typically, only low-power (<100-mW) operation is necessary.

The collection optics limit the light reaching the detector to that scattered at 90° from a small volume (~0.2 x 0.2 x 0.2 mm). It is

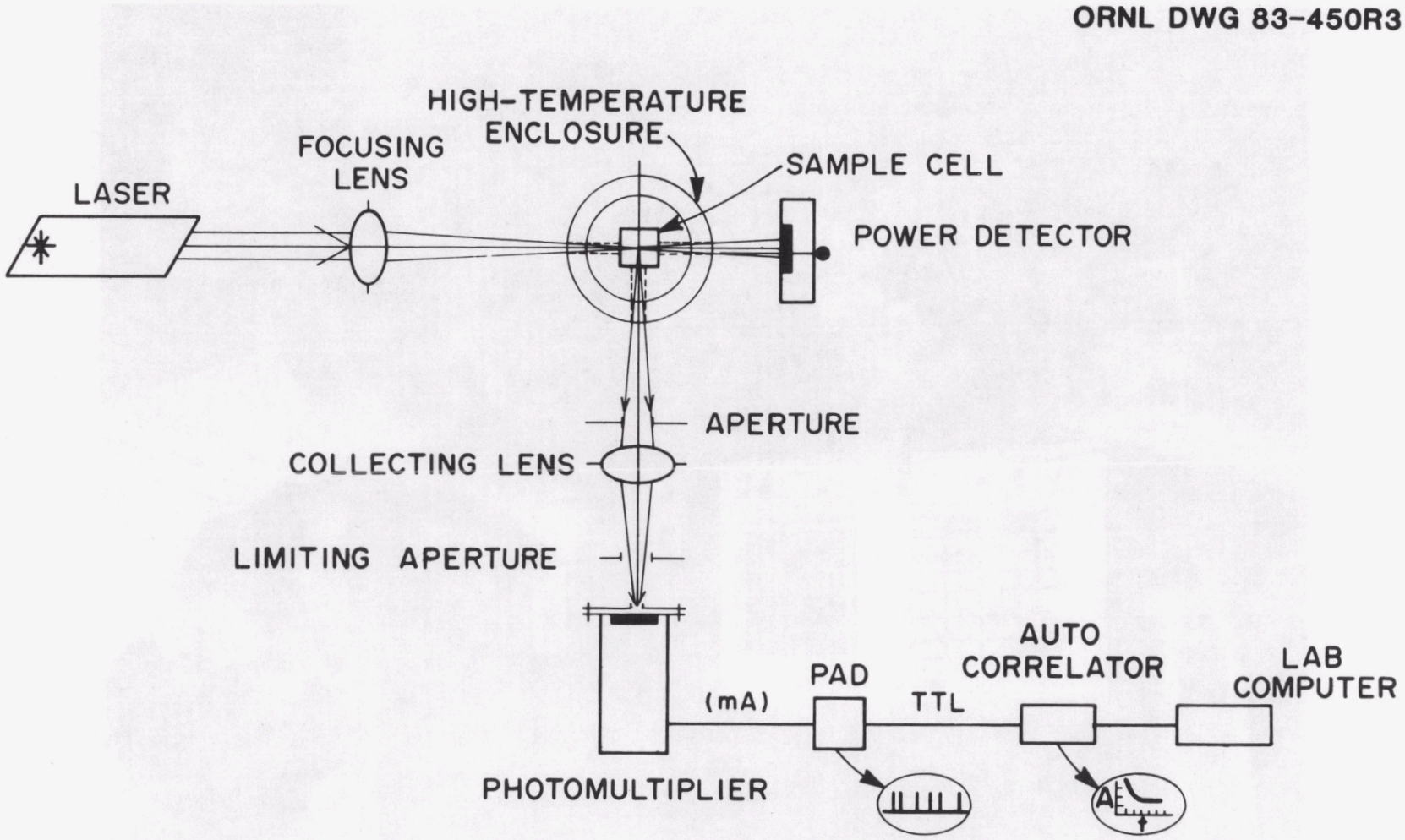

Fig. 5. Dynamic light-scattering spectrometer for high-temperature experiments.

ORNL-PHOTO 6319-84

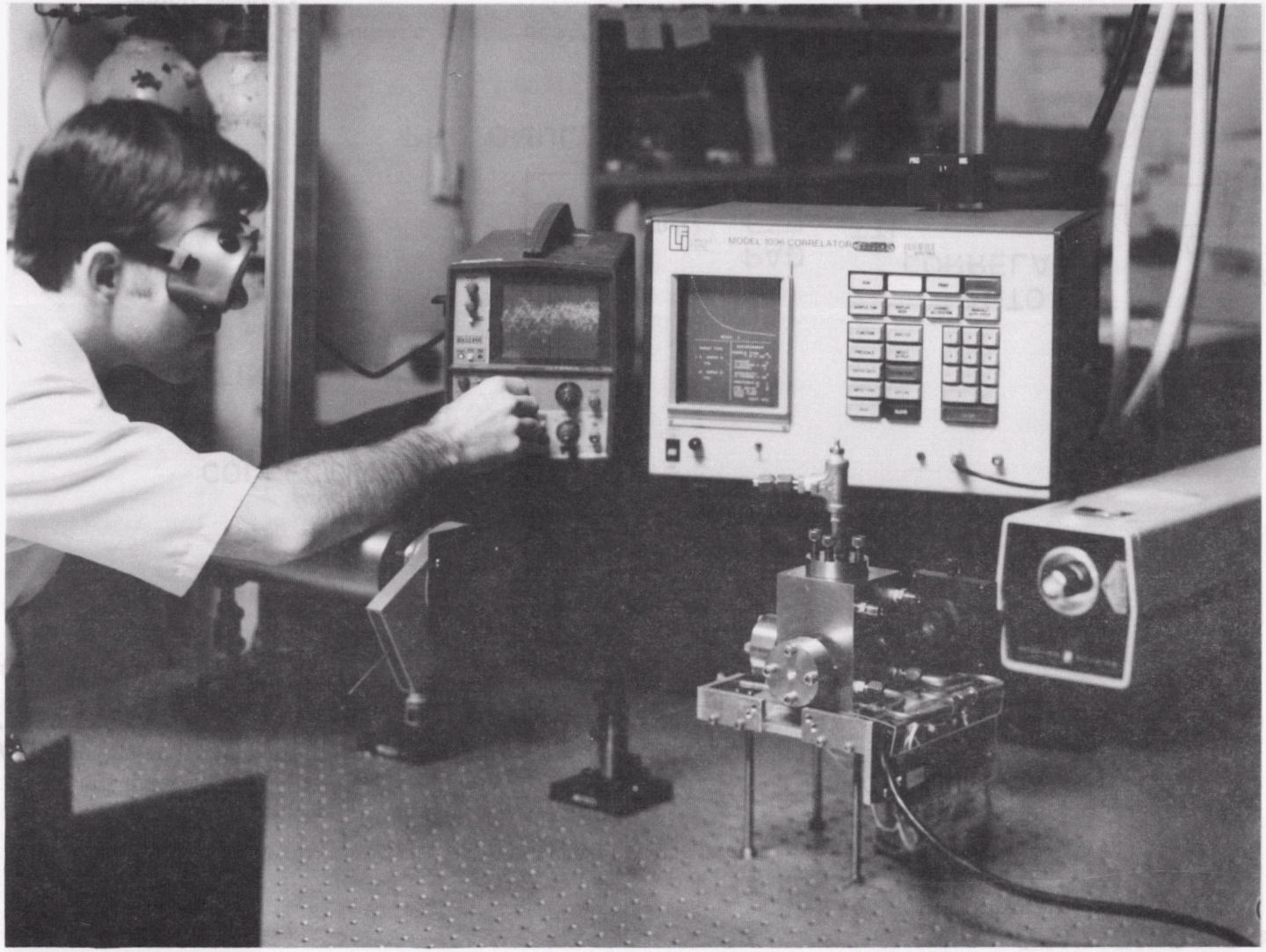

Fig. 6. Operation of high-temperature spectrometer.

important that the scattering volume be kept sufficiently small to ensure the coherence of the light reaching the detector. Incoherent light does not contribute to the signal due to the destructive interference of components of different phase. Guidelines for the sizing and placement of the limiting apertures have been reviewed in several articles.[13,17,18] The first aperture is a small iris diaphragm (0.68 mm, Ealing No. 22-3305), which is located just in front of the imaging lens. A 100-mm plano-convex lens is placed approximately 8 in. from the center of the sample cell. The final aperture is a precision adjustable slit (Oriel No. 7250, 0- to 3.2-mm opening, ±0.1 mm) which is mounted vertically, just in front of the detector and in the plane of the image formed by the lens. All of the components are positioned along the axis normal to both the incident beam and the plane of polarization.

The detector is an end-window photomultiplier (EMI No. 9863B350) mounted in a housing that provides radio frequency and magnetic shielding (Pacific model 3262 RF). A stable power supply (Pacific model 204-03) generates the 2000-V dc potential required for the photomultiplier (PMT). A photon striking the cathode behind the PMT entrance window causes an electron to be emitted. This electrical signal is enhanced by a factor of 10^6 in the subsequent dynode-multiplier section. Figure 6 illustrates the nature of the fluctuating PMT signal (on the oscilloscope) and the resulting exponential autocorrelation function.

The pulse amplifier discriminator (PAD, Langley Ford model PD-01) converts the milliamp pulses generated by the PMT to TTL pulses (0-5 V, dc) for use in a digital correlator. Pulses due to spurious effects in the PMT are also eliminated by the PAD.

The autocorrelator (Langely Ford model 1096) is a sophisticated digital signal processor that can accurately approximate the ideal autocorrelation function given by Eq. (8). Details of the electronic and mathematical operations are given in the literature.[7,28] The time scale that can be probed ranges from decay periods of 1 μs to 10 s. A RS-232 communications interface between the autocorrelator and a microcomputer (Apple IIe) permits automated operation, off-line analysis, and convenient data logging. Data and calculated results are stored on magnetic disks.

The method for preparing an alcosol was developed by Stober.[24] In this method, a monodisperse silica sol is formed by the controlled hydrolysis of ethyl orthosilicate [$Si(OC_2H_5)_4$, EOS] in an alcohol-ammonia-water mixture. TEOS is hydrolyzed in the presence of water, with ammonia acting as a catalyst. In a typical preparation, 5.4 mL of concentrated NH_4OH (28% NH_3) and 85 mL of absolute ethanol are mixed in a clean flask. Then, TEOS is added (3.54 g), and the resulting reaction mixture is poured partially into a flask and partially into a clean quartz spectrophotometer cell.

Observations were made at ambient temperature for the initial experiments discussed here. The reaction mixture in the cell was placed in its holder, and the laser-light-scattering data were acquired continuously for the time during which the growth of particles occurred. Generally, this was a several-hour period. A bluish-white opalescence, indicating the presence of submicron particles, could normally be observed within 15 min. For the concentrations noted earlier, a terminal spherical particle diameter of 0.1 μm was obtained.

The portion of the mixture that remained in the flask was analyzed for ethanol, using a Tracor 550 gas chromatograph equipped with a flame-ionization unit. A glass column packed with 1% SP1000 on 80/100 Carbopac C was used to separate the species involved in the reactions. Obviously, accurate analyses were not possible in the cases where ethanol was used as the solvent.

5. RESULTS AND DISCUSSION

Several observations were made during this phase of the study of the controlled crystallization of oxide species. They can be summarized as follows:

1. The effects of water and ammonia concentration on the growth rate of silica, as well as the ultimate diameter of the particle, were studied at ambient temperature.
2. The effect of diluting the reactant concentration on the ultimate diameter of the silica, as determined by laser-light scattering, was measured.
3. The solvent was changed as its effect on the kinetics of the reaction and on the particulate growth was observed.

In the initial experiments, our objective was to explore the effects of the water and ammonia concentrations on the growth rate of silica in an ethanol solvent. Figure 7 shows experimental results for two typical runs in the series. The diameter of the silica spheres is given as a function of time. An electronmicrograph for one of the runs in this series (see Fig. 8) shows some dispersity. A particle size distribution, taken manually from a large field of this photograph (Fig. 9) confirms that there was dispersity in the 0.03- to 0.08-μm range. Because of the basic

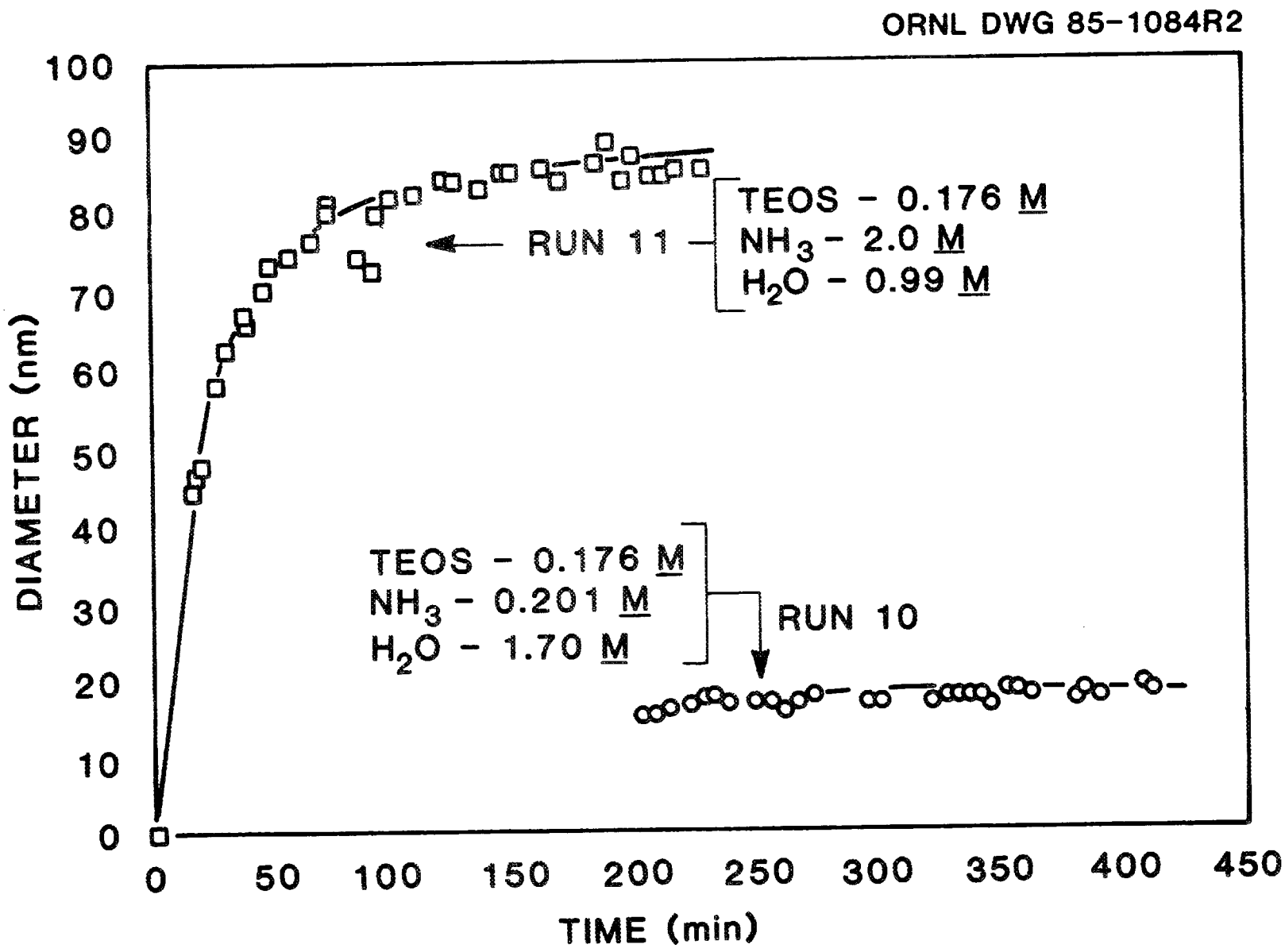

Fig. 7. Effects of NH_3 and H_2O on silica growth in ethanol medium.

ORNL-PHOTO 6062-84

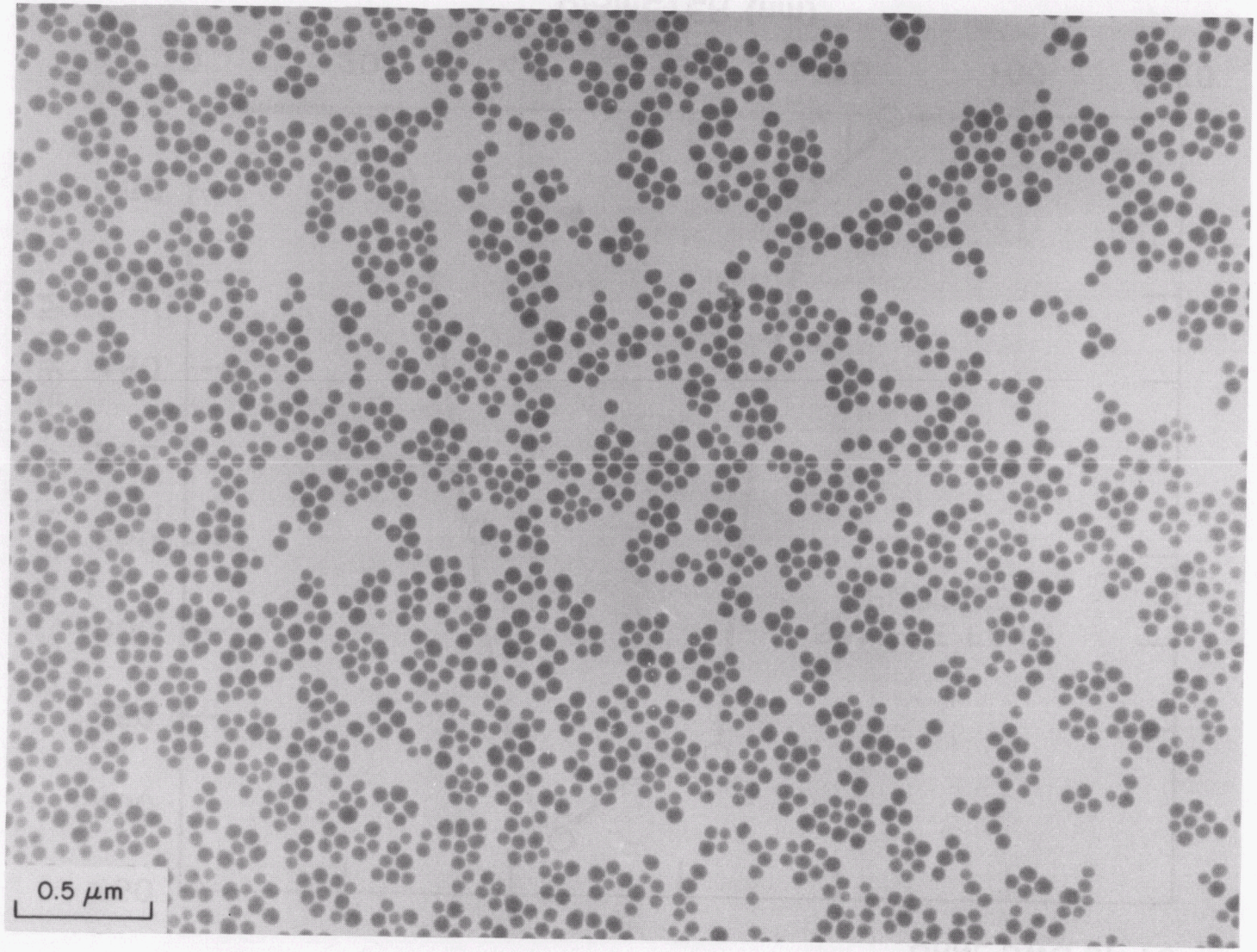

Fig. 8. Colloidal silica produced by controlled hydrolysis in ethanol (Stöber process). Conditions: stock F91; temperature = 25°C.

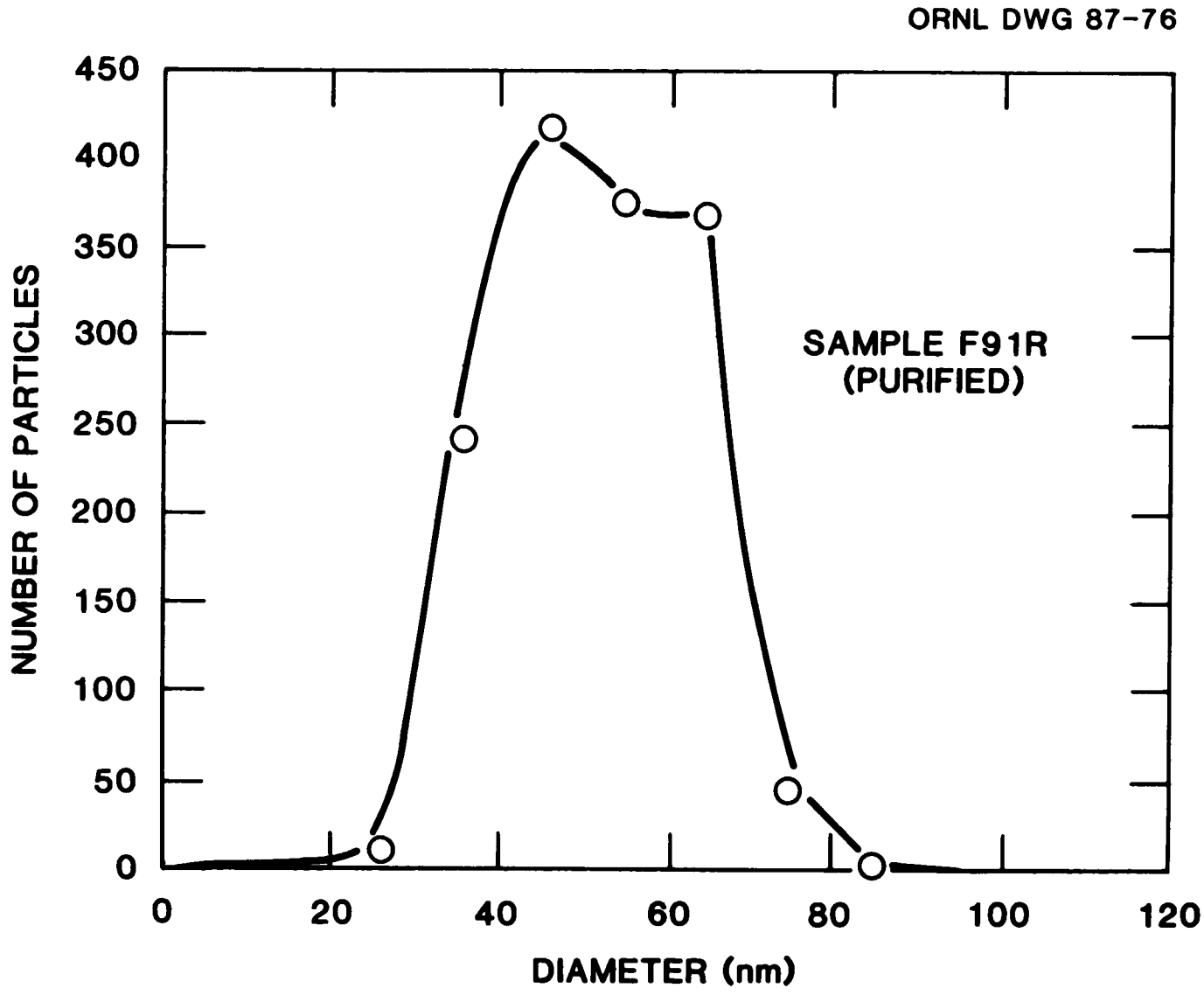

Fig. 9. Size distribution.

differences in the means of assessing particle sizes between electron microscopy and in situ laser-light scattering, a comparison of the results of the two methods can only be qualitative. In spite of the differences, however, the diameters found by scattering are within 10% of those found by electron microscopy, which is well within the expected range. Intensity results were also taken for each of the runs in the series (see Fig. 10). If the particles are monodispersed, one can eventually compute the number of particles in the mixture from intensity results and hence assess the time dependency of growth in the number of particles in the dispersion. The study is obviously limited to dilute systems in which multiple scattering does not significantly contribute to the scattered signal.

The effect of diluting the totally reacted silica suspensions on the size of particles, which is computed by the laser-light-scattering experiment, was investigated. Dilution of the suspension with anhydrous ethanol led to a substantial increase in the observed average particle diameter as a function of dilution (see Fig. 11). The 12% increase in diameter is significant experimentally and led to other dilution studies, first with ethanol saturated with ammonia (2.5 M) and then with ethanol containing ammonia at a concentration equal to that of the original solution. Increasing the ammonia concentration in the solution appeared to decrease diameters, while a steady ammonia concentration gave constant diameter results. Since the value computed by the program for the diameter is dependent on the viscosity and the refractive index of the medium, it appears reasonable to assume that a variation of physical properties could account for the results reported in Fig. 11.

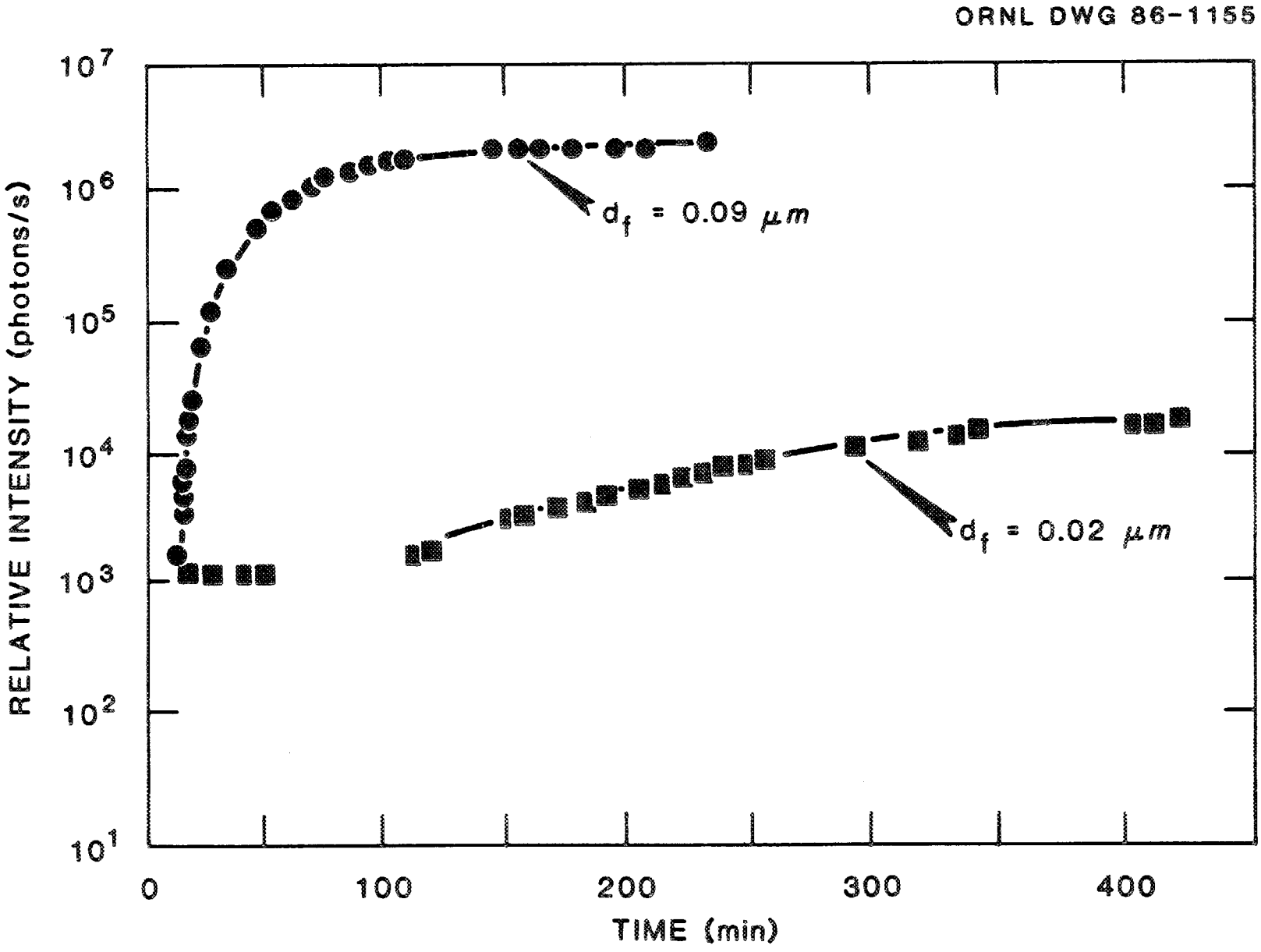

Fig. 10. Intensity of scattered light (large and small particles).

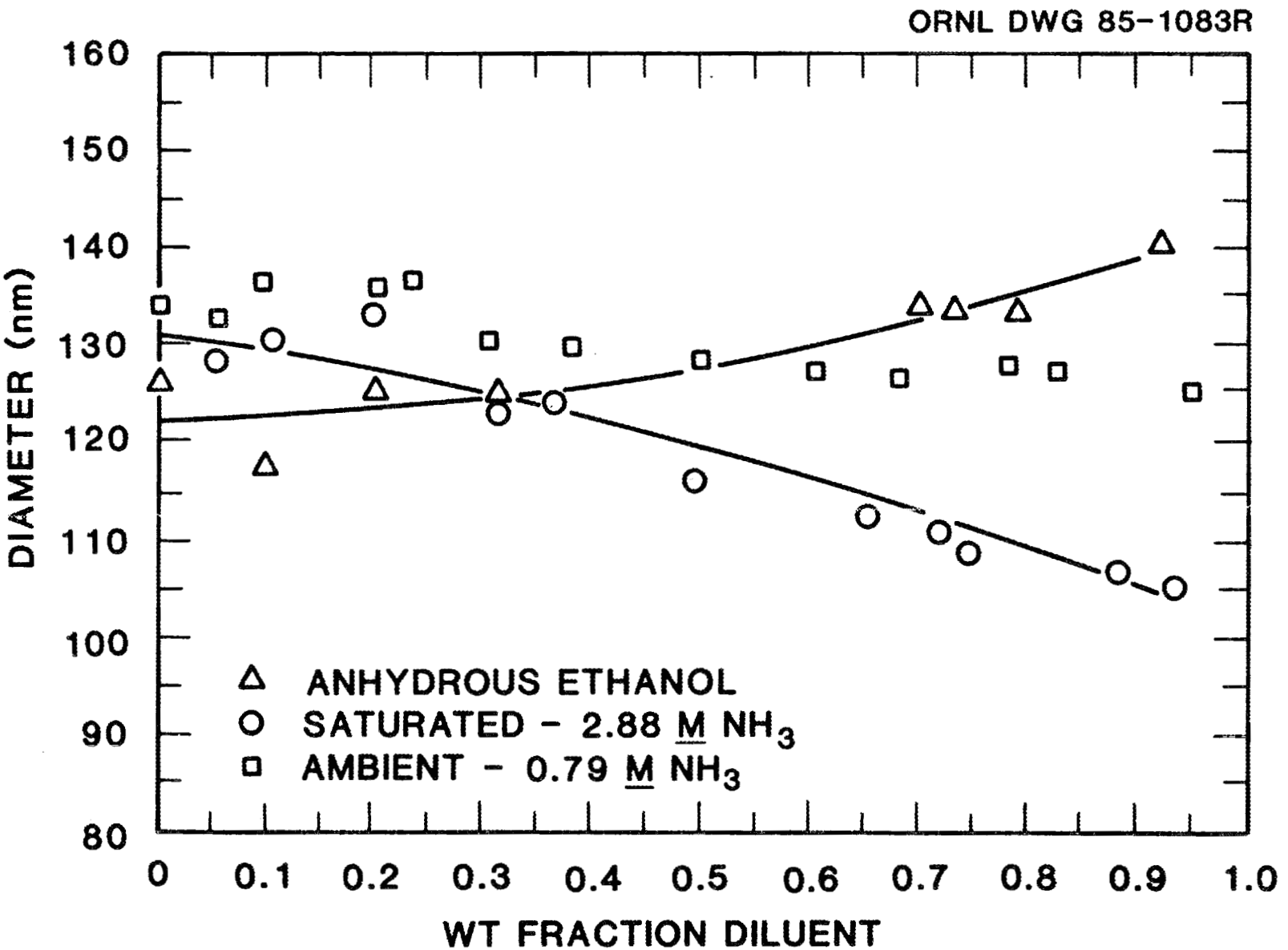

Fig. 11. Dilution of silica suspensions with ethanol and NH_3-ethanol.

As a part of this program, some scoping studies were undertaken to assess the effects of the three participants in the reaction on the ultimate size of the particles. The results are summarized in Table 1. The objective of these studies was to grow particles in the size range of interest for the equipment that is available (0.02 to 0.5 μm). Insufficient data were taken to allow an assessment of the effect of TEOS concentration. The influence of the other two species was to produce larger particles when either was increased. Hydrolysis was very slow in the absence of the catalyst. Stober[24] showed that one could make particles in the 1- to 2-μm size range by using a higher concentration of TEOS; in that case, there was a maximum size beyond which higher water

Table 1. Effects of initial reactant concentrations on ultimate diameter of the particles

Initial reactant concentrations (M)			Diameter (μm)
TEOS	NH_3	H_2O	
0.135	0.816	1.66	0.12
0.176	0.800	1.7	0.12
---	---	---	---
0.176	0.2	1.7	0.03
0.176	0.80	1.7	0.120
0.176	2.00	1.66	0.175
---	---	---	---
0.176	2.00	0.99	0.09
0.176	2.00	1.66	0.175
0.176	2.00	2.54	0.35

concentrations resulted in the production of smaller particles, presumably as a result of a higher initial population of nuclei. In each study, an increased ammonia concentration resulted in faster reactions and larger nuclei. Ultimately, the initial solution became saturated with ammonia.

In addition to the reactants and catalyst, the solvent appears to have a significant effect on the behavior of the system. A series of runs in which all the conditions of the reaction were identical, except for the solvent used, was performed with ethanol, n-butanol, and tert-butyl alcohol. The results of these experiments are shown in Fig. 12. The ultimate size of the particles was found to increase with increasing molecular weight and with the progression from normal to tertiary alcohols. In fact, the particles grew so large in the tert-butyl alcohol case that sedimentation of the particles substantially undermined the experiment. Since roughly the same amount of material was converted to silica in each experiment, many more nuclei must be formed in ethanol than in the butanols. It is possible that steric factors are responsible for some of this effect. Certainly, further investigation along these lines is warranted.

The kinetics of the reaction may be followed by monitoring the water content and the amount of ethanol produced during the process, as well as the mass of particles precipitated. Since relatively small amounts of ethanol are formed, it is important to use a different alcohol as the solvent. It has been shown that the ethoxy group exchanges slowly with all but the tertiary alcohols.[27] Therefore, we selected tert-butyl alcohol as the solvent for the kinetic studies. The ethanol produced in a run is monitored with a gas chromatograph; hence, the use of a higher-molecular-weight alcohol was advantageous. Figure 13 is a typical electronmicrograph

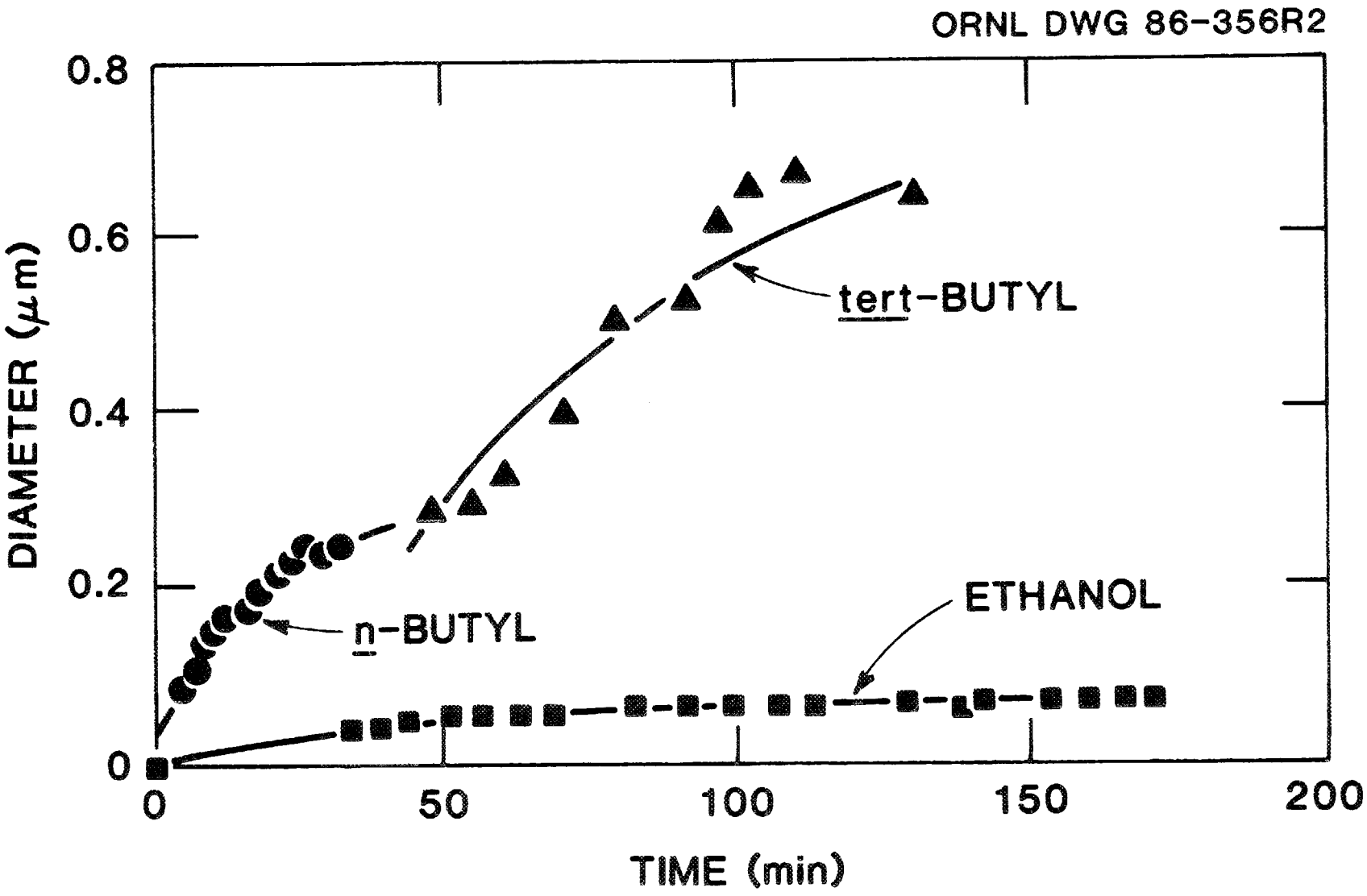

Fig. 12. Effect of solvent on silica growth rate.

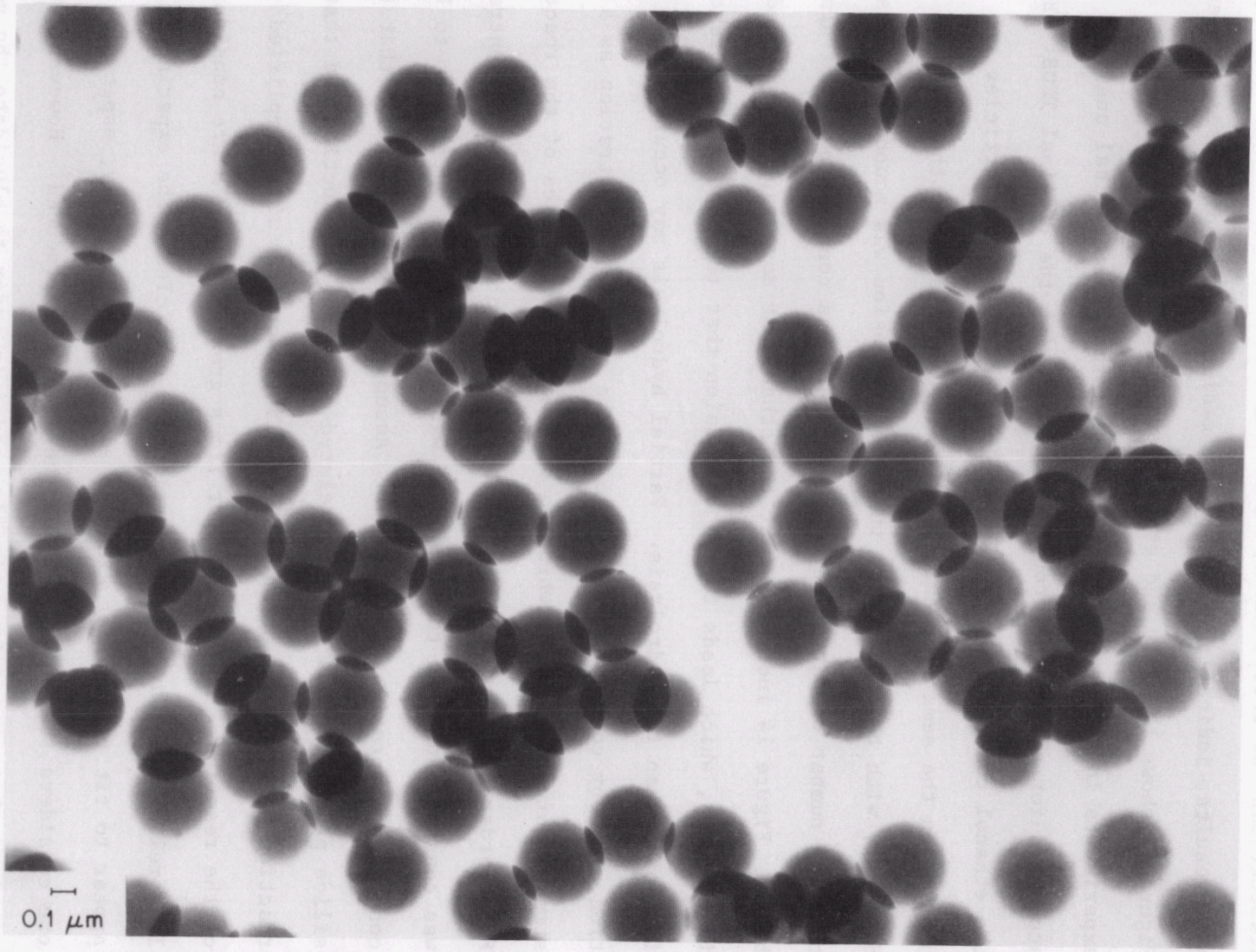

Fig. 13. Silica particles formed by hydrolysis of TEOS in tert-butyl alcohol.

of silica produced in tert-butyl alcohol. The photograph agrees with the diameter size as determined by laser-light scattering and the polydispersity results, indicating an excellent medium for monodispersed studies. Figure 14 shows the size and ethanol production data for one of the experiments in the series. The ethanol formed in the final analysis accounted for all of the groups associated with the original TEOS. Both the ethanol concentration and the volume of the single particles are plotted on the same time axis. The volume was based on the measured diameter, with the assumption that the suspension was monodispersed and that the number of particles in the mixture was constant and well distributed. Figure 14 indicated that the ethanol is more rapidly produced than is the SiO_2, which leads to the conclusion that the condensation reaction is slower than the hydrolysis. Partial hydrolysis may occur in this reaction, thereby complicating the use of the ethanol concentration as a straightforward basis on which to determine the kinetics of the reaction. First-order kinetics were tested, assuming that the ammonia concentration was constant and that the amount of water present was sufficient to be considered approximately constant. Assumptions were also made that the silica production was directly related to ethanol production and that the reaction went to completion. Figure 15 illustrates this simplified view of the reaction. The results for times greater than 3 h are considered less reliable because of the settling of particles. The experimental data appear to fit first-order kinetics almost quantitatively, especially when one considers the basis on which the graph was produced. However, we conclude that more information is needed in order to elucidate the mechanism. The development of means for measuring the silica concentration as well as the water concentration will be important in future experiments.

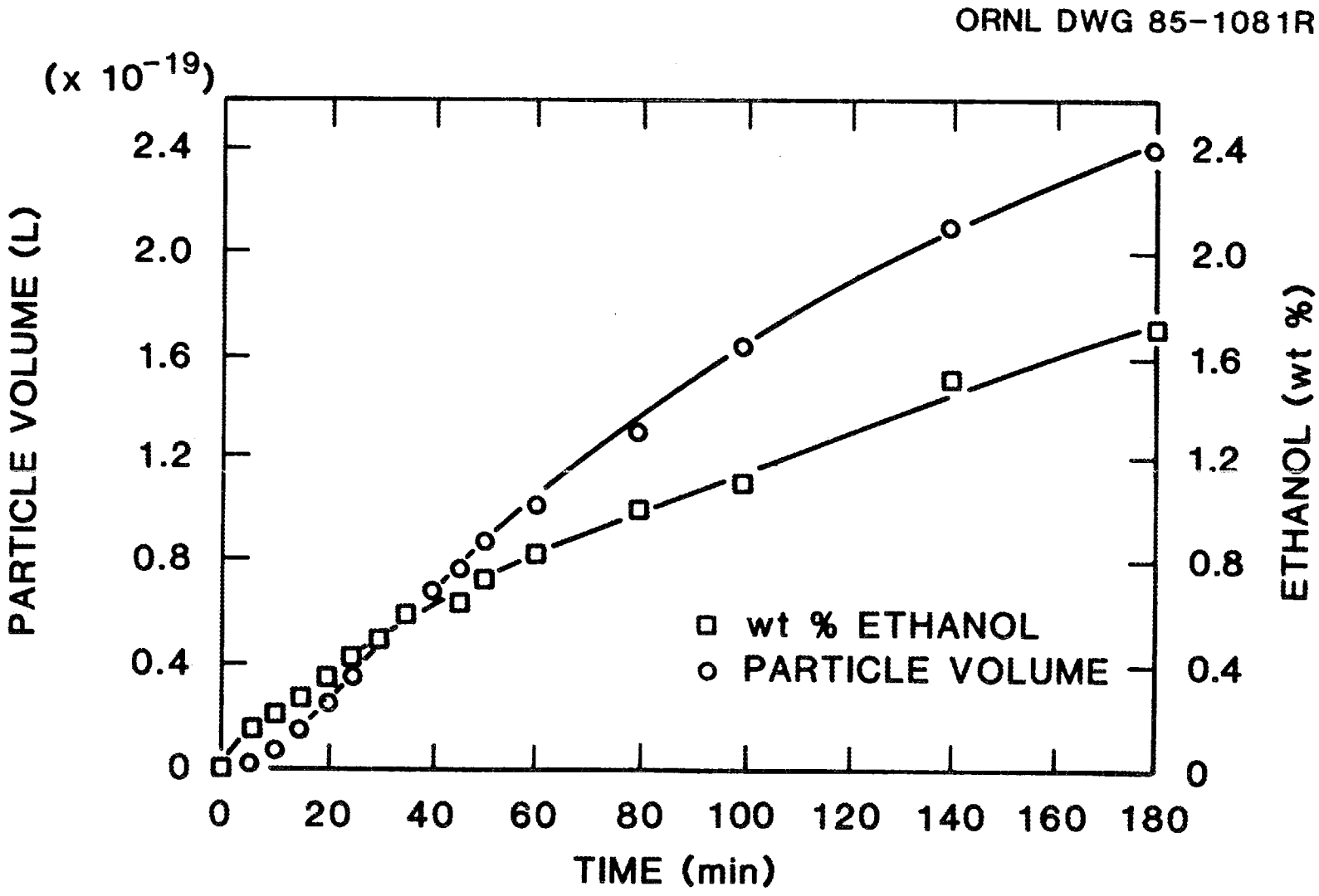

Fig. 14. Hydrolysis of TEOS-Run 41; variation of wt % ETOH and particle volume with time.

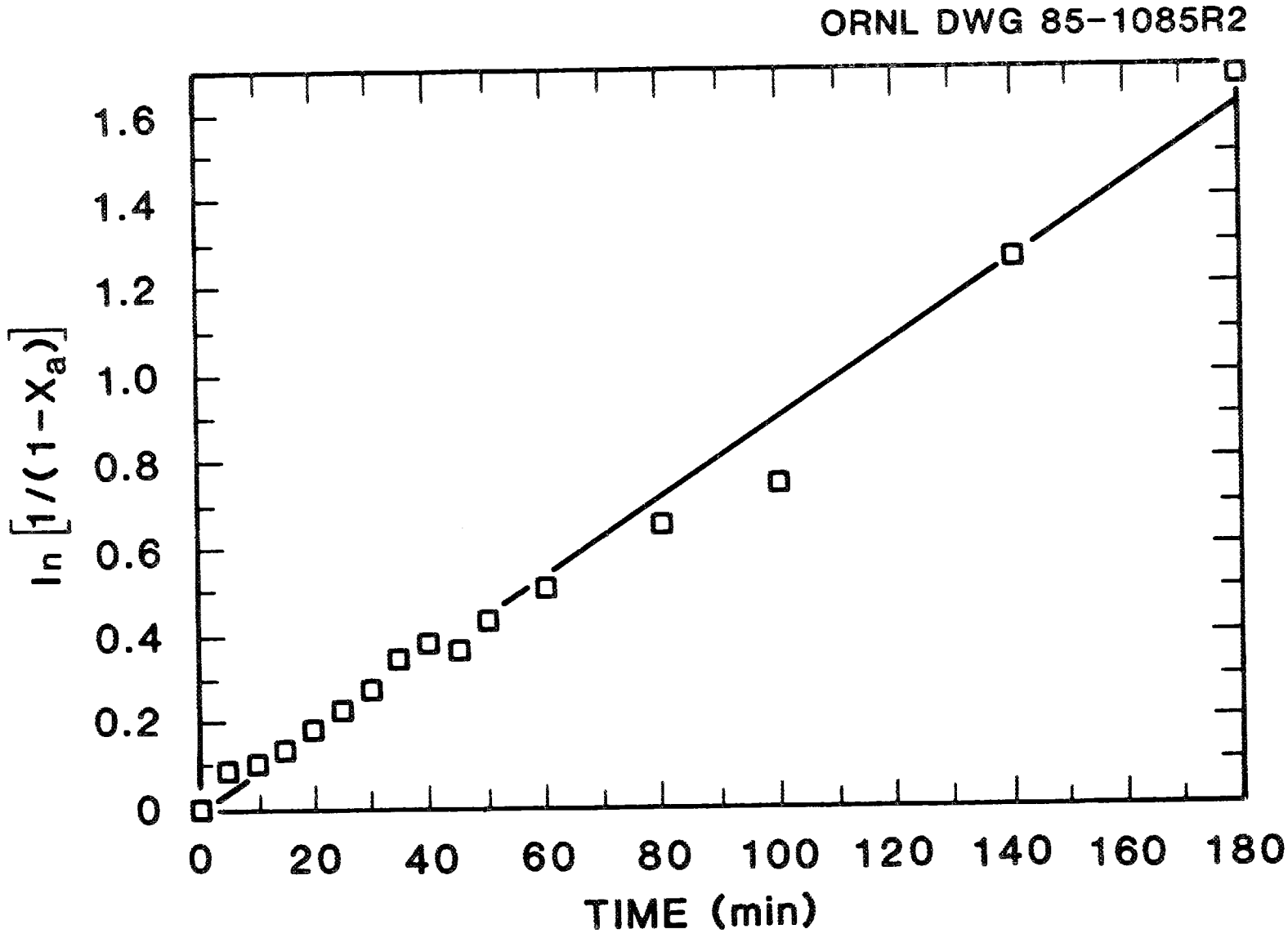

Fig. 15. Hydrolysis of TEOS-Run 41; first-order kinetics.

6. CONCLUSIONS

The combination of homogeneous nucleation and in situ crystallization in a laser-light-scattering system provides a convenient way of observing controlled precipitation and crystallization in the 0.005- to 1-μm region. The resulting information will provide insight into the basic mechanisms associated with crystallization.

The precipitation of silica from TEOS provides an excellent model system with which to work. The information gathered on silica is of both fundamental importance and practical interest in the production of glasses and advanced ceramics. Preliminary results with the system show that monodisperse particles are formed, with growth being controlled by the reactants, the catalyst, and the medium in which the reaction occurs. The formation rate of the silica appears to be first order with respect to TEOS concentration.

Observation of systems in the 0.001- to 0.005-μm region with light scattering will be feasible if small scattering angles are used.

7. NOMENCLATURE

$A(t)$ - arbitrary signal; continuous function of time

$\overline{A}(t)$ - fluctuating influence of molecular collisions on particle motion

$A^*(\tau)$ - time-domain autocorrelation function of $A(t)$ (heterodyne)

$A^*(\omega)$ - frequency-domain scattering results

D - self-diffusion coefficient = $kT/(6\pi a\eta)$

$E_s(t)$ - scattered electric field

K - arbitrary constant

M - molecular weight

N - number of particles in scattering volume

N_i - concentration of polymer with molecular weight M_i

$P(q,r)$ - Mie scattering factor

$P(\bar{u}_o)$ - probability of occurrence of velocity $\bar{u}_o$

T - temperature (absolute)

$W(x,y;z)$ - probability of occurrence of x and y, given z

a - particle radius

d_p - particle diameter

$f(r)$ - normal distribution of particles

k - Boltzmann's constant

m - particle mass

n - refractive index of the medium

$\bar{q}$ - scattered field vector = vector difference between incident and scattered propagation vectors

$\bar{r}$ - position vector

t - time

$\bar{u}$ - velocity vector

Greek Letters

β - coefficient of dynamic friction $\sim (6\pi a\eta)/m$

Γ - linewidth (Hz), half-width at half-height of frequency-domain autocorrelation function $\sim q^2D$ (heterodyne case) or $\sim 2q^2D$ (homodyne)

η - shear viscosity

θ - scattering angle

λ - wavelength of light

μ_n - moment of distribution, order n

τ - time increment

τ_c - characteristic decay time of autocorrelation function

Subscripts

i - incident condition or compound index

j - summation index, over jth condition, interval particle, or compound

o - initial or original condition

s - scattered condition

8. REFERENCES

1. R. E. Lerch and R. E. Norman, "Fuel Conversion and Fabrication Chemistry," presented at the American Chemical Society Meeting, Seattle, Wash., Mar. 20-25, 1983; to be published in Radiochim. Acta.

2. General Electric Co., Research and Development Requirements for Conversion Processing Alternatives, NEDG-21951, San Jose, Calif., 1978.

3. H. K. Bowen, "Basic Research Needs on High Temperature Ceramics for Energy Applications," Mater. Sci. Eng. 44(1), 1-56 (1980).

4. DOE, Topical Basic Energy Sciences Meeting (Materials Science), "Characterization and Behavior of Submicron Nitride and Carbide Powder," Albuquerque, N. Mex., Mar. 1-2, 1984.

5. Alan Randolph, ed., "Design, Control, and Analysis of Crystallization Processes," AIChE Symp. Ser. No. 193 76 (1980).

6. Nyult Jaroslov, Industrial Crystallization: State of the Art, Verlog Chemie, Deerfield Beach, Fla., 1982.

7. Barton Dahneke, ed., Measurement of Suspended Particles Using Quasi-Elastic Light Scattering, Wiley, New York, 1982.

8. D. F. Williams, "Determination of High Temperature Fluid Viscosity Using Dynamic Light Scattering," M.S. Thesis, University of Tennessee, Knoxville, March 1985.

9. S. W. Provencher, "CONTIN: A General Purpose Constrained Regularization Program for Inverting Noisy Linear Algebraic and Integral Equations," Comput. Phys. Commun. 27, 229-42 (1982).

10. Egon Matijevic, "Monodispersed Metal (Hydrous) Oxides - A Fascinating Field of Colloid Science," Acc. Chem. Res. 14(1), 22-29 (1981).

11. Egon Matijevic, "Preparation and Characterization of Monodispersed Metal Hydrous Oxides Sols," Prog. Colloid Polym. Sci. 61, 24-35 (1976).

12. A. K. Van Helden et al., "Preparation and Characterization of Spherical Monodisperse Silica Dispersions in Nonaqueous Solvents," J. Colloid Interface Sci. 18(2), 354-68 (June 1981).

13. B. J. Berne and R. Pecora, Dynamic Light Scattering, Wiley, New York, 1976.

14. S. Chandrasekhar, "Stochastic Problems in Physics and Astronomy," Rev. Mod. Phys. 15(1), 1-89 (1943).

15. B. Crosignoni et al., Statistical Properties of Scattered Light, Academic Press, New York, 1975.

16. A. Einstein, Ann. d. Physik 17, 549 (1906).

17. B. Chu, Laser Light Scattering, Academic Press, New York, 1974.

18. B. Dahneke, ed., Measurement of Suspended Particles by Quasi-Elastic Light Scattering, Wiley, New York, 1983.

19. J. C. Brown and P. N. Pusey, "Photon Correlation Study of Polydisperse Samples in Cyclohexane," J. Chem. Phys. 62(3), 1136-44 (1975).

20. C. B. Bargeron, "Measurement of a Continuous Distribution of Spherical Particles by Intensity Correlation Spectroscopy: Analysis by Cumulants," J. Chem. Phys. 61(5), 2134-38 (1974).

21. D. E. Koppel, "Analysis of Macromolecular Polydispersity in Intensity Correlation Spectroscopy: The Method of Cumulants," J. Chem. Phys. 57(11), 4184-20 (1972).

22. Masataka Ozaki and Egon Matijevic, "Preparation and Magnetic Properties of Monodispersed Spindle-Type γ-Fe_2O_3 Particles," J. Colloid Interface Sci. 107, 199-203 (1985).

23. August Janeković and Egon Matijevic, "Preparation of Monodispersed Colloidal Cadmium Compounds," J. Colloid Interface Sci. 103, 436-47 (1985).

24. Werner Stober et al., "Controlled Growth of Monodisperse Silica Spheres in the Micron Size Range," J. Colloid Interface Sci. 26, 62-69 (1968).

25. B. E. Yoldas, "Formation of Titania-Silica Glasses by Low Temperature Chemical Polymerization," J. Noncryst. Solids 38-39, 81-86 (1979).

26. B. W. Peace and K. G. Mahan, "Polymers from the Hydrolysis of Tetraethoxysilane," Polymer 14, 417 (1973).

27. A. Voij, "Light Scattering by Dispersions of Model Colloids," Colloid Interface Sci. 16, 139-41 (1982).

28. E. Jakeman, "Theory of Optical Spectroscopy by Digital Autocorrelation of Photon Counting Fluctuations," J. Phys. A. 3, 201-15 (1970).

INTERNAL DISTRIBUTION

1. P. F. Becher
2. J. M. Begovich
3. A. Bieier
4. W. D. Bond
5-7. R. R. Brunson
8-12. C. H. Byers
13. H. D. Cochran
14-18. M. T. Harris
19. J. R. Hightower
20. F. R. Mynatt
21. C. D. Scott
22. T. C. Scott
23. S. A. Sherrow
24. J. S. Watson
25. R. M. Wham
26. R. G. Wymer
27. Central Research Library
28. Y-12 Technical Library, Document Reference Section
29-30. Laboratory Records
31. Laboratory Records, R.C.
32. ORNL Patent Section

EXTERNAL DISTRIBUTION

33. H. Jones, Battelle Northwest Laboratories, P.O. Box 999, 300 Area/320 Building, Richland, WA 99352

34. J. J. Perona, Department of Chemical Engineering, University of Tennessee, Knoxville, TN 37916

35-39. D. F. Williams, Department of Chemical Engineering, University of Washington, Seattle, WA 98105

40. I. L. Thomas, Office of Basic Energy Sciences, DOE, Mail Station J-321, GTN, Washington, D.C. 20545

41. Office of Assistant Manager for Energy Research and Development, U.S. Department of Energy — ORO, Oak Ridge, TN 37831

42-71. Technical Information Center, Oak Ridge, TN 37830